TURBULENCE MEASUREMENTS FOR A NEAR-FIELD POLLUTANTS DISPERSION CAMPAIGN IN A STRATIFIED SURFACE LAYER

Xiao Wei*, Eric Dupont, Bertrand Carissimo, Eric Gilbert, Luc Musson-Genon

1. INTRODUCTION

Pollutants dispersion in a stable atmospheric boundary layer and in complex environment is still a phenomenon that is relatively poorly described by modeling and difficult to reproduce in a wind tunnel. Nevertheless, this topic is of major interest in the field of air pollution from human activities such as industrial risks and road transportation, as stable conditions induce large fluctuations of pollutants concentrations with possible occurrence of very high values. An experimental program consisting in measuring pollutants dispersion in a stratified surface layer and in near-field (less than 200m) is carried out on the site SIRTA (Instrumental Site Research by Atmospheric Remote Sensing), on the campus of the Ecole Polytechnique, about 20 km south of Paris.

Before implantation of SIRTA program, a literature study was made on previous campaigns conducted by other research groups in the world, including several campaigns organized by Met Office in UK (Mylne and Mason, 1991; Mylne 1992; Mylne et al. 1996), the urban dispersion experiment MUST (Mock Urban setting Test) (Biltoft C.A., 2002) and the CASES-99 Field Experiment (Poulos G.S. et al., 2002) both held in US. It appears that the subject of pollutant dispersion in an urban environment has been fairly well documented, and measurements were made on spatial scales ranging from several hundred meters to a few kilometers. However, there are campaigns such as CASES-99 in which the surface boundary layer has been studied in detail during strong thermal stability situations but without understanding through the dispersion of pollutants. Conversely, some campaigns were well documented in terms of pollutant concentration measurements, but contained very little dynamic measurement, for example campaigns described in Mylne 1992. As for the MUST experiment, although its studies have validated flow dynamics and pollutants dispersion in some near neutral atmospheric stratification in idealized urban field, this measurement campaign was not designed to study small-scale atmospheric turbulence in stable thermal stratification and associated dispersion. Taking into account the literature review, the aim of the SIRTA program has been defined to characterize the fine structure of turbulence and associated dispersion through collocated high temporal and spatial resolution measurements. These measurements are performed through an extensive network of ultrasonic anemometers measuring wind turbulence and through photo-ionization detectors measuring concentration of a tracer gas.

Background elements of SIRTA experimental program is introduced in section 2. Impact of terrain heterogeneity on the turbulence especially on wind direction is described in section 3. Section 4 presents several results in turbulence data processing and analysis from an intensive observation period (IOP). Section 5 summarizes the present study and future work.

2. DESCRIPTION OF THE EXPERIMENTAL PROGRAM

The objectives for SIRTA turbulence and dispersion study have been defined as document simultaneously, in high temporal and spatial resolution and in near field, wind fluctuations and concentration fluctuations of a tracer gas. This data set should allow analyzing the concentration fluctuations in relation with the characteristics in time and space of the turbulence field. The main features of the campaign are:

- Experiment in near field (50 to 200 m);
- Focus on stable thermal stratification, but may include some neutral stratification or slightly convective situations;
- High frequency measurements (about 10Hz) to cover the entire frequency spectrum of fluctuations;
- Large number of sensors measuring turbulence and concentration of tracer gas to document spatial inhomogeneities.

Figure 1(a) shows the whole measurement area in SIRTA field. Our campaign is carried out in Zone 1 which is limited in the north by a forest and

* *Corresponding author address:* Xiao Wei, CEREA (Atmospheric Environment Teaching and Research Centre, Joint Laboratory Ecole des Ponts ParisTech/EDF R&D, Université Paris-Est), EDF R&D, 6 quai Watier, 78401 Chatou, France. Email: xiao.wei@edf.fr

in the south by a road. A lot of instruments are operated in routine mode on this site (Haeffelin et al., 2005) and there were already some interesting experiments carried out on this site which can inspire us in data analysis (Fesquet, 2008) and in modeling (Zaïdi et al., 2013). In future, it will be possible to study the effects of an idealized building by adding a container on the downstream side of the gas release point on the site.

(a)

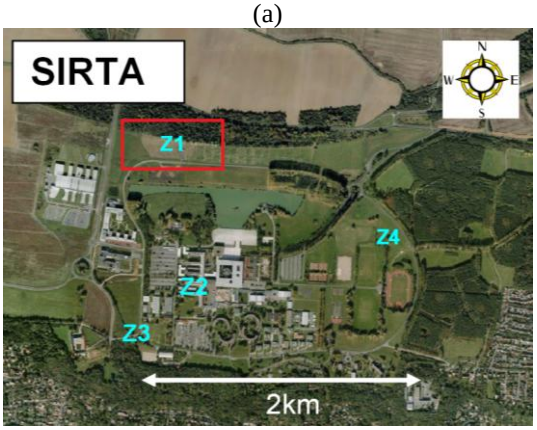

(b)

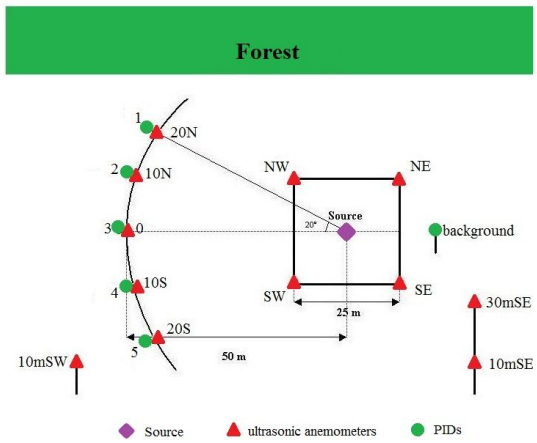

Figure 1. (a) Whole measurement area in the SIRTA field and (b) sensors position in Zone 1.

Several specific meteorological conditions are required to perform the tracer experiment. After a climatology study based on data between April 2007 and September 2009 on the site, we finally choose criteria as follows:

- As the measurement zone is oriented along the east-west axis, wind direction must be such that plume is transported from dissemination point to the instrumented area, which means that wind direction must be between 75° and 105°, being closest to 90° (easterly wind).
- Wind velocity must be between 0.5 and 5 ms^{-1}, in order to stay in unfavorable dispersion conditions.
- Temperature difference *T*(30m) - *T*(10m) and Monin-Obukhov length must be positive, assuring to be in stable stratification.
- Relative humidity should be less than about 90% to avoid excessive condensation on sensors measuring tracer gas concentration.

Concerning the experimental devices, dynamic measurements are mainly provided by ultrasonic anemometers, measuring three components of wind velocity (*u, v, w*) (in meteorological reference) and sound velocity (from which is derived the “sonic” air temperature *T*) at 10 Hz. Propylene is chosen as the tracer gas because of its low toxicity, low boiling point, low cost and low ionization potential. Photo-ionization detector (PID) is chosen to measure the gas concentration at 50 Hz, because of its good sensitivity to propylene. Turbulence measurements have been recorded continuously for more than two years (since April 2012), while concentration measurements have been performed only during short (about 1 hour) releases of gas for specific meteorological conditions (tracer tests).

Figure 1(b) shows position of sensors used for the experiment. Red triangles (▲) represent ultrasonic anemometers. There are four of them placed respectively at four corners of a square of side 25m centered on the release point (◆). They are named according to their positions: NE (northeast), NW (northwest), SE (southeast) and SW (southwest). We denote them as "sonic square" in the following. There are five anemometers arranged in a circle arc with radius 50m, centred on the source. They are named according to the angle with respect to the east-west axis as 20N, 10N, 0, 10S and 20S. We denote them as "sonic arc at 50m" in the following. All the nine anemometers are at height of 3m. In addition, there is another ultrasonic anemometer at the top of a 10 m tower in the southwest of the field which is called "10mSW". Similarly, for the other two ultrasonic anemometers at heights of 10 m and 30 m on a 30 m tower in the southeast of the field, they are named "10mSE" and "30mSE". Green dots (●) represent the PIDs. There are five of them collocated with the five ultrasonic anemometers at "sonic arc at 50m". They are numbered from north to south by 1, 2, 3, 4 and 5. Another PID is positioned upstream of the source to measure background concentration and it is called “background”. To resume, turbulence is measured at three levels (3 m, 10 m and 30 m height) with an intensive network at 3 m height, and concentration is measured only at height of 3 m.

3. IMPACT OF TERRAIN HETEROGENEITY

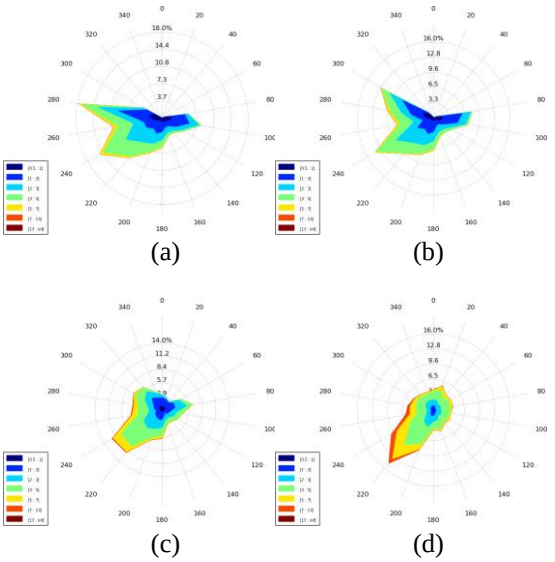

Figure 2. Wind rose from measurements over two years (April 2012 – March 2014) for anemometers (a) NE, (b) SE, (c) 10mSW and (d) 30mSE.

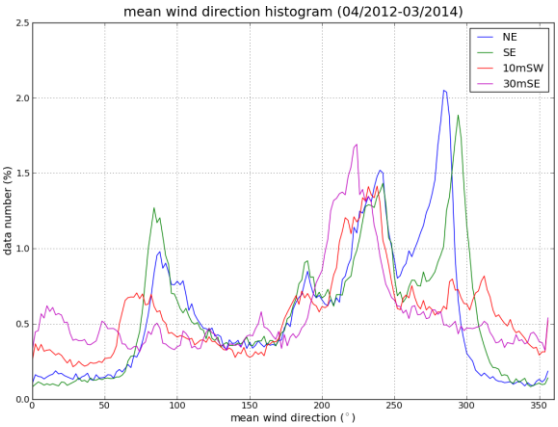

Figure 3. Mean wind direction histogram from measurements over two years (April 2012 – March 2014) at three levels: 3m (NE and SE), 10m (10mSW) and 30m (30mSE).

Site heterogeneity plays an important role for turbulence in Zone 1. In particular, the forest to the north modifies the wind velocity and direction for a large northerly sector. Figure 2 shows wind roses for measurements over two years (April 2012 – March 2014) at three levels: 3 m (NE and SE), 10 m (10mSW) and 30 m (30mSE). We can see clearly the different wind rose form between measurements at height of 3 m and 30 m. At 3 m height, wind velocity is much smaller and there is almost no wind for a large northerly sector. There's also a slight difference between two wind roses of anemometers at 3 m height, especially for westerly sector. Wind measured by anemometer SE is more from north-west than that measured by anemometer NE. We also plot histograms of mean wind direction deduced from the same measurements of the same anemometers at three levels. As the forest has a height of 15 m, its perturbation affects especially the measurements at lower levels. Histogram of anemometer 30mSE implies that the prevailing wind direction on the site is south-west (around 230°). As for lower levels, except peak at prevailing wind direction, some new peaks appear around 90° and 270°, particularly for the measurements at 3 m height. Moreover, histograms of anemometers NE and SE show that there are very few winds for a large northerly sector (0° - 60° and 300° - 360°), which is consistent with wind roses. This phenomenon is due to wind channeling effect from the forest to the north of the instrumented area. This channeling effect can be found only below the forest height, the wind direction above the canopy seems to remain unaffected.

4. TURBULENCE STUDY FOR MEASUREMENTS DURING IOP

Intensive observation periods (IOPs) with gas releases have been performed since March 2012. A 60 min sub-period (from 19:08 to 20:08) from an IOP on 5th June 2013 (from 18:48 to 20:17) has been chosen here to present data analysis results.

4.1 Statistics

Variables such as mean wind direction dd_{mean} and velocity a_{mean}, variances of the 3 wind components $(\sigma_a^2, \sigma_b^2, \sigma_w^2)$, turbulent kinetic energy *TKE*, friction velocity u_*, vertical heat flux Q_0 and Monin-Obukhov length L_{MO}, are reported in table 1, in which a and b are streamwise and crosswind components of the velocity, and *dd* is the horizontal wind direction. They have been calculated over the sub-period of 60 min in the IOP on 5th June 2013 during which meteorological conditions are almost stationary.

The statistical values for anemometers at same level generally agreed well with each other. The three variances show that the flow measured is strongly anisotropic. The positive values of L_{MO} indicate that the measurement period is clearly a stable stratification situation. It has also been checked with the vertical temperature gradient. The mean wind velocity measured by anemometers on the south is always greater than that measured on

the north, and the mean wind direction also has a lag between measurements from anemometers on the north and on the south. These are due to the northern forest which slows down wind velocity and reorients wind direction. Wind directions measured at higher levels are much more north-east than that at height of 3m, which is consistent with the observations presented in the previous paragraph. Also L_{MO} increases with height in such a way that z/L_{MO} is roughly constant.

	NE	NW	SE	SW	20N	10N	0	10S	20S	10mSW	10mSE	30mSE
dd_{mean} (°)	111.5	106.8	95.0	96.1	108.0	94.1	94.9	90.2	92.4	75.4	71.7	58.2
a_{mean} (ms^{-1})	0.92	1.00	1.63	1.83	1.22	1.39	1.43	1.59	1.68	2.06	2.42	3.54
σ_a^2 (m²s^{-2})	0.44	0.53	0.54	0.61	0.48	0.50	0.61	0.51	0.56	0.67	0.81	1.29
σ_b^2 (m²s^{-2})	0.30	0.33	0.50	0.49	0.38	0.40	0.42	0.48	0.48	0.52	0.52	0.77
σ_w^2 (m²s^{-2})	0.10	0.12	0.13	0.13	0.11	0.13	0.14	0.14	0.14	0.25	0.25	0.32
TKE(m²s^{-2})	0.42	0.49	0.59	0.61	0.49	0.51	0.59	0.56	0.59	0.72	0.79	1.19
u_* (ms^{-1})	0.21	0.23	0.26	0.25	0.22	0.23	0.24	0.25	0.28	0.36	0.37	0.53
Q_0 (Kms^{-1})	-0.03	-0.06	-0.03	-0.06	-0.03	-0.03	-0.04	-0.04	-0.05	-0.02	-0.03	-0.03
L_{MO} (m)	21	16	40	20	24	26	24	31	34	176	131	416
L_{aa} (m)	14.82	13.13	14.86	16.69	19.62	19.67	19.50	13.99	14.28	33.31	-	91.95
L_{bb} (m)	5.67	6.42	11.11	12.47	7.68	9.56	8.46	10.81	12.27	11.51	16.00	24.76
L_{ww} (m)	1.83	2.00	1.96	2.02	2.07	2.08	2.15	2.07	2.35	5.96	7.27	8.84

Table 1. Statistical values of 12 anemometers calculated from the 60 min sub-period data of the IOP on 5 June 2013.

	θ (°)	U (ms^{-1})	$U_{adv\,a}$ (ms^{-1})	$U_{adv\,b}$ (ms^{-1})	$U_{adv\,w}$ (ms^{-1})	r_a	r_b	r_w
(NE, NW)	19.1	0.96	2.53	2.71	-	2.64	2.82	-
(SE, SW)	5.6	1.73	2.82	2.28	2.37	1.63	1.32	1.37
(NW,10N)	16.4	1.47	2.13	2.15	2.01	1.45	1.46	1.37
(NW, 20N)	9.4	1.11	1.42	1.49	-	1.28	1.34	-
(SW, 10S)	2.7	1.71	2.60	2.03	-	1.52	1.19	-
(SW, 20S)	11.9	1.76	2.35	2.56	-	1.34	1.45	-

Table 2. Comparison between mean wind speed and eddy advection speed deducted from spatial cross-correlation, where r_a , r_b and r_w are ratios of the eddy advection velocity to the mean wind speed $r=U_{adv}/U$ for three wind velocity components.

4.2 Integral length scale

We deduct also integral length scales L from velocity autocorrelation with $L= a_{mean}T_e$, where T_e is an integral time scale obtained with approximation that T_e equals to the time lag where the autocorrelation coefficient goes below e^{-1} for the first time. Integral length scales of three wind velocity components L_{aa} , L_{bb} and L_{ww} have different order of magnitude (see table 1) which shows again that turbulence near the ground is strongly anisotropic in stable conditions. They have also greater values with increasing altitude which implies that turbulence has lager eddies at higher levels.

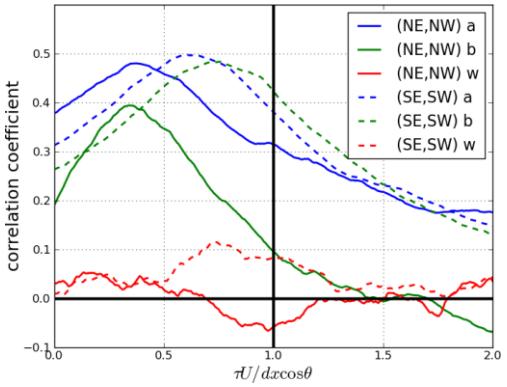

Figure 4. Spatial cross-correlation of anemometers couples (NE, NW) and (SE, SW) as a function of normalized time lag.

4.3 Velocity cross-correlation

The spatial cross correlation of velocity is a useful tool for examining the validity of Taylor's hypothesis and for determining the eddy advection velocity (Powell and Elderkin, 1974).

Figure 4 plots the cross-correlation coefficients of anemometers couples (NE, NW) and (SE, SW) as a function of normalised time lag $\tau U/dx\cos\theta$, where U is the average mean wind speed of two correlated anemometers, dx is the distance between them, and θ is the deviation of the mean wind direction from a direction parallel to their separation

(Horst *et al.* 2004). The cross-correlation peak reaches up to 0.5 for streamwise component, whereas vertical components are poorly correlated. Theoretically, the cross-correlation peak should centred at $\tau U/dx\cos\theta = 1$. However, they are all on the left of the vertical line at $\tau U/dx\cos\theta = 1$. Defining the eddy advection velocity as $U_{adv} = dx\cos\theta/\tau_{max}$, where τ_{max} is the time lag at the maximum correlation, the curves in figure 4 imply that U_{adv} is higher than the mean wind speed U measured directly by the anemometers at the same level. Table 2 compares the mean wind speed and eddy advection speed deducted from spatial cross-correlation, and a ratio of the eddy advection velocity to the mean wind speed is estimated as $r=U_{adv}/U$. We notice that U_{adv} is always much greater than U. Similar results were found in HATS (Horizontal Array Turbulence Study) field program (Horst *et al.* 2004), but their difference between these two velocities is smaller than ours. Explanation of the fact that ratio $r>1$ can be that there is a strong vertical velocity gradient in the surface layer near the ground, and eddy advection is probably affected by the flow at higher level where velocity is larger than that at height of 3 m. Moreover, it is possible that Taylor's hypothesis is not valid during the experiment which means that eddies evolve faster than they travel the distance between two correlated anemometers. The velocity cross-correlation at higher level for anemometers (10mSE, 10mSW) is very noisy, probably due to the large distance (about 120 m) between them.

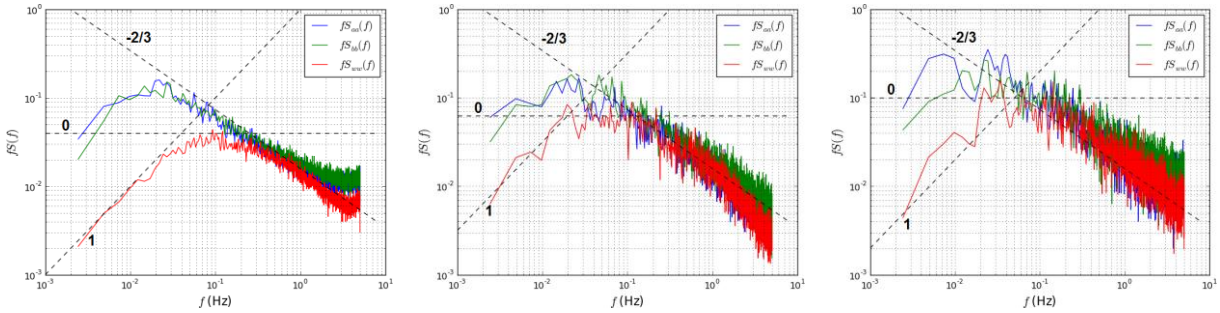

Figure 5. Velocity power spectra $f\,S(f)$ at heights of 3 m (left), 10 m (middle) and 30 m (right), calculated by the average spectra of anemometers at the same level.

4.4 Power spectra

Power spectrum is another way to study turbulence structure. In a first step, we compared the *TKE* power spectra with Kolmogorov's theory which implies the existence of an inertial subrange in the spectra. However, instead of following the -5/3 power law, a slope between -1 and -5/3 is found if we consider the whole spectral interval between the low frequency peak and 1 Hz. Since there are many studies made on different velocity components spectra, we plotted the three velocity components power spectra at heights of 3 m, 10 m and 30 m (figure 4). The spectra showed are the average spectra of anemometers at the same level, so the spectra at height of 30 m and 10 m are much more fluctuating than those at height of 3 m because of fewer sensors at these levels. We observe that for the high frequency region there is the expected inertial subrange for all the spectra. For the lower frequency region, there is a frequency lag in spectrum form between vertical velocity and horizontal ones showing strong anisotropy of turbulence, which is enhanced by the stable stratification. The vertical velocity spectrum is increasingly close to the others with increasing height, which means a less anisotropic turbulence at higher levels.

According to Carlotti and Drobinski (2004) and Drobinski *et al.* (2004), very close to the ground, there is a layer dominated both by shear and blocking by the ground which is called the eddy surface layer. In this layer, eddies coming from upper layers are stretched along the wind direction, thus losing their isotropy, and a k_1^{-1} subrange can be observed in velocity spectra for horizontal components of the velocity. Richard et al. (1997), Hunt and Morrison (2000) and Högström et al.(2002) had all illustrated the existence of k_1^{-1} subrange for horizontal velocity spectra and found that the extension of this self-similar range decreases with increasing height owing to the decreasing effects of shear-sheltering. In our horizontal velocity spectra, the plateau at lower frequency range to the inertial subrange seems to have roughly a 0 slope which shows the existence of the self-similar k_1^{-1} subrange. Unfortunately, our spectra is too fluctuating and don't extent enough in low frequency region to see clearly the lower limit of the k_1^{-1} subrange. We can still find that the upper limit of this range decreases with increasing height,

which has been pointed out by Högström et al. (2002).

Vertical velocity spectra have been shown to have a different form with horizontal velocity spectra by the above mentioned papers. At lower frequency region, a range where $S_{33}(f) \propto u_*^2 z$ has been proposed by Drobinski *et al.* (2004). We find that our vertical velocity spectra respect well a slope 1 corresponding to a range $fS_{33}(f) \propto f$ prior to the power spectra peak, which is consistent with the typical form of vertical velocity spectra in surface layer. The low frequency part of spectra seems to increase with height, as indicated in Högström et al. (2002) in the surface layer. However, some evidence of a k_1^{-1} subrange can also be found at intermediate frequency range in vertical velocity spectra especially at height of 3 m. The origin of this phenomenon is still unknown, as all the theories have been made under near-neutral conditions, while our measurements are made under stable ones which might cause an eddy surface layer much thinner. So it's possible that our measurements are made in a transition zone of eddy surface layer and shear surface layer above. Also, the forest and shelters around might change in complex ways the flow by creating other shear layers and mixing them with eddy surface layer.

5. Summary

In this paper we have briefly presented a turbulence study for a near-field pollutants dispersion campaign in a stable surface layer. We first described the flow heterogeneity by illustrating the wind channelling effect of the forest to the north of the instrumented area. The forest modifies the wind velocity and changes the wind direction especially for the flow beneath its height. Then, we characterized the turbulence in the surface layer near the ground by calculating variances, integral length scales and spectra for the three velocity components. Turbulence strong anisotropy is quantified by different order of magnitude between variances $(\sigma_a^2, \sigma_b^2, \sigma_w^2)$ and integral length scales (L_{aa}, L_{bb}, L_{ww}) in our stable surface layer. From spatial velocity cross-correlation, we have deduced an eddy advection velocity greater than the mean wind velocity measured directly by anemometers at the same level. In spectral study, we found correspondence between literatures and our measurements for horizontal and vertical velocity spectra form, and some evidence of a k_1^{-1} subrange in spectra of all the velocity components which shows the existence of an eddy surface layer very close to the ground.

In the future, turbulence data analysis will be made on continues measurements over 2 years in order to study the dependence of turbulence characteristics on stability (from near-neutral to very stable). Several more PIDs are arriving which will allow to extend the instrumental set-up. With concentration data analysis, relationships between turbulence and concentration fluctuations are expected to be found. Finally all this data set will allow detailed comparisons in different configurations with numerical simulations which have been carried out with the open source CFD code Code_Saturne co-developed at CEREA and Electricité de France (EDF), with different turbulence modeling levels and with Eulerian and Lagrangian dispersion.

References

Biltoft, C.A., 2002: customer report for Mock Urban Setting Test. West Desert Test Center, U.S Army Dugway Proving Ground, Report WDTC-FR-01-121.

Carlotti, P. and Drobinski, P., 2004: Length scales in wall-bounded high-Reynolds-number turbulence. *Journal of Fluid Mechanics*., 516, 239-264.

Drobinski, P., Carlotti, P., Newsom, R.K., Banta, R.M., Foster, R.C. and Redelsperger, J., 2004: The Structure of the Near-Neutral Atmospheric Surface Layer. *Journal of the Atmospheric Sciences*, 61, 699–714.

Fesquet, C., 2008 : Structure de la turbulence atmosphérique à proximité de la surface. PhD thesis, l'Ecole Polytechnique.

Haeffelin, M. et al., 2005: SIRTA, a ground-based atmospheric observatory for cloud and aerosol research. *Annales Geophysicae*, 23: 253-3275.

Högström, U., Hunt, J. C. R. and Smedman, A. S., 2002: Theory and measurements for turbulence spectra and variances in the atmospheric neutral surface layer. Bound.-Layer Meteor., 103, 101–124.

Horst, T.W., Klessl, J. and Lenshow, D.H., 2004: HATS: Field Observations to Obtain Spatially Filtered Turbulence Fields from Crosswind Arrays of Sonic Anemometers in the Atmospheric Surface Layer. *Journal of the Atmospheric Sciences*, 61, 1566-1581.

Hunt, J.C.R. and Morrison, J. F., 2000: Eddy structure in turbulent boundary layers. Eur. J. Mech. B/Fluids, 19, 673–694.

Mylne, K.R., 1992: Concentration Fluctuation Measurements in a Plume Dispersing in a Stable Surface Layer. *Boundary Layer Meteorology*, 60, 15–48.

Mylne, K.R. and Mason, P.J., 1991: Concentration fluctuation measurements in a dispersing plume at a range of up to 1000 m. Quarterly Journal of the Royal Meteorological Society, 117, 177–206.

Mylne, K.R., Davidson, M.J. and Thomson, D.J., 1996: Concentration fluctuation measurements in tracer plumes using high and low frequency response detectors. *Boundary Layer Meteorology*, 79, 225–242.

Poulos, G.S., W. Blumen, D.C. Fritts, J.K. Lundquist, J. Sun, S.P. Burns, C. Nappo, R.M.

Banta, R.K. Newsom, J. Cuxart, E. Terradellas, B. Balsley, and M. Jensen, 2002: CASES-99, A Comprehensive Investigation of the Stable Nocturnal Boundary Layer, *Bull. Amer. Meteorol. Soc.* 83**,** 555-581.

Powell, D.C. and Elderkin, C.E., 1974: An Investigation of the Application of Taylor's Hypothesis to Atmospheric Boundary Layer Turbulence. *Journal of the Atmospheric Sciences*, 31, 990-1002.

Richards, P. J., Fong, S. and Hoxey, R. P., 1997: Anisotropic turbulence in the atmospheric surface layer. J. Wind Eng. Ind. Aerodyn.,69–71, 903–913.

Zaïdi, H., Dupont, E., Milliez, M., Musson-Genon, L. and Carissimo, B., 2013: Numerical simulations of the microscale heterogeneities of turbulence observed on a complex site. *Boundary Layer Meteorology*, 147, 237-259.